Annals of Biomedical Engineering
https://doi.org/10.1007/s10439-024-03570-5

BMES BIOMEDICAL ENGINEERING SOCIETY

ORIGINAL ARTICLE

Expanded Combined Loading Injury Criterion for the Human Lumbar Spine Under Dynamic Compression

Maria Ortiz-Paparoni[1] · Joost Op 't Eynde[1] · Christopher Eckersley[1] · Concetta Morino[2] · Mitchell Abrams[1] · Derek Pang[1] · Jason Kait[1] · Frank Pintar[3] · Narayan Yoganandan[4] · Jason Moore[4] · David Barnes[5] · Kathryn Loftis[6] · Cameron R. Bass[1]

Received: 29 November 2023 / Accepted: 24 June 2024

Abstract

Contemporary injury tolerance of the lumbar spine for under-body blast references axial compression and bending moments in a limited range. Since injuries often occur in a wider range of flexion and extension with increased moment contribution, this study expands a previously proposed combined loading injury criterion for the lumbar spine. Fifteen cadaveric lumbar spine failure tests with greater magnitudes of eccentric loading were incorporated into an existing injury criterion to augment its applicability and a combined loading injury risk model was proposed by means of survival analysis. A loglogistic distribution was the most representative of injury risk, resulting in optimized critical values of $F_{r,\mathrm{crit}} = 6011$ N, and $M_{\mathrm{y,crit}} = 904$ Nm for the proposed combined loading metric. The 50% probability of injury resulted in a combined loading metric value of 1, with 0.59 and 1.7 corresponding to 5 and 95% injury risk, respectively. The inclusion of eccentric loaded specimens resulted in an increased contribution of the bending moment relative to the previously investigated flexion/extension range (previous $M_{\mathrm{y,crit}} = 1155$ Nm), with the contribution of the resultant sagittal force reduced by nearly 200 N (previous $F_{r,\mathrm{crit}} = 5824$ N). The new critical values reflect an expanded flexion/extension range of applicability of the previously proposed combined loading injury criterion for the human lumbar spine during dynamic compression.

Keywords Lumbar spine · Combined loading · Dynamic compression · Survival analysis · Injury probability

Introduction

Acute injuries to the lumbar spine often stem from falls, vehicular accidents, and sports-related incidents, with research worldwide consistently identifying the lumbar spine as a prevalent area for spinal fractures [4, 10, 13, 26]. In examining military populations, lumbar spine injuries are the fourth most prominent injury in vehicle occupants wounded in action, and second most prominent in vehicle occupants killed in action during an under-body blast (UBB) event [12, 16]. Further, lumbar spine injuries during dynamic compression have been highly prevalent in recent American military conflicts in part due to the increased use of improvised explosive devices [2, 3, 7]. Determining the human injury tolerance of the lumbar spine has been a vital step for the development of effective injury mitigation efforts, such as the US Army-sponsored Warrior Injury Assessment Manikin (WIAMan) [11], with lumbar spine injuries in dynamic scenarios being investigated through Hybrid III dummies [32] and cadaveric lumbar spines [5, 23]. Particularly, through studies that investigate the axial force injury tolerance for the lumbar spine during UBB [31] and the first generation of a combined loading metric tolerance for a limited range of occupant's seated postures [14]. However, to expand the range of applicability of a combined loading injury criterion, a wider range of postures that further flex or extend the lumbar spine needs to be investigated. Elucidating the relationships between spinal compression and flexion with injury tolerance may be applicable in civilian contexts such as automotive accidents, specifically frontal crashes, building upon recent studies also incorporating evaluation of flexion and compression in the literature [25].

During an UBB event, the rapid compressive loading of the lumbar spine can be coupled with bending moments, depending on the occupant's seated position and weight

Associate Editor Steven Rowson oversaw the review of this article.

Extended author information available on the last page of the article

Published online: 06 September 2024

distribution [22], which can lead to differences in loading patterns that then exacerbate the injury outcome [33]. While previous studies have determined an injury tolerance of lumbar vertebral body fracture due to axial compression alone [23, 30, 31], injury risk is highly dependent on the complex geometry of the spine and the loading path of the forcing event, which is likely not purely axial in most scenarios. The dynamic nature of events with emphasized underbody forces and complex loading patterns, such as UBB, motor vehicle accidents, pilot ejections, and rotary wing incidents, pose significant challenges for modeling and predicting injuries. Therefore, a combined loading metric is essential for accurately describing injury risk. The versatility of a combined metric allows the integration of the mechanical effects of various forces and moments acting on the lumbar spine, providing a comprehensive assessment of the injury risk. Recent studies have examined the effect of combined flexion and compression in the lumbar spine on 75 male human cadaveric lumbar spines under UBB [14] and additionally on 40 cadaveric lumbar spine segments modeling injury in the context of automotive crashes, seeing clinically relevant vertebral fractures in 21 specimens [25]. The combined loading injury criterion proposed by Ortiz-Paparoni et al.[14] was developed for nominal driver or passenger seated postures that were obtained from body segment or seat angles and anthropometric data from the University of Michigan Transportation Research Institute (UMTRI) Seated Soldier Study, assessing 310 individuals encumbered with varying clothing or equipment [17]. However, to further elucidate and capture the contributions of the bending moment to the lumbar spine injury risk it is imperative to consider a wider range of postures that expands beyond the nominal and standard deviation range of postures of the Seated Soldier Study. Therefore, this study aims to expand the previously established combined loading lumbar injury criterion (LIC) by including a broader range of seated postures and accounting for a greater contribution of the bending moment, leading to the development of an "expanded combined loading injury criterion" (ECLIC).

Materials and Methods

To expand the range of assessed seated postures from the original 75 specimens, fifteen unembalmed cadaveric lumbar spines in four additional postures were subjected to high-rate dynamic compressive loading. The postures were defined as Army Combat Uniform (ACU) reclined, intermediate, flexed reclined, and flexed nominal posture (Fig. 1) derived from the Seated Soldier with ACU Study [17]. All cadaveric testing was performed in compliance with Duke University's Institutional Review Board experimental cadaver protocols.

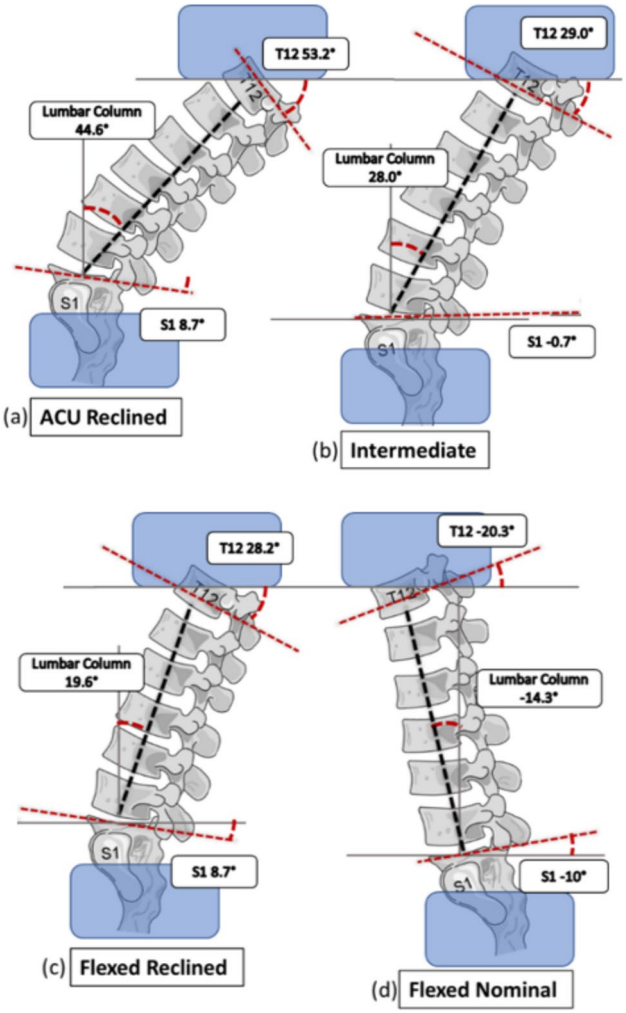

Fig. 1 Expanded range of postures based on the Seated Soldier Study. **a** ACU reclined. **b** Intermediate. **c** Flexed reclined. **d** Flexed nominal

To effectively incorporate the 15 specimens to the existing data set, preparation and test procedures were followed to replicate those established in Ortiz-Paparoni et al. [14]. Prior to testing, specimens were preserved frozen at − 20 °C and left to thaw at room temperature for 24 h prior to preparation. Selection of specimens was performed to exclude any samples with joint degradation or osteophytes through assessment via microCT imaging performed at 100 × 100 × 100 µm resolution (Model XTH 225 ST, Nikon Metrology Inc., Brighton, MI, USA) to preserve a representative mechanical response. Further, specimen acceptance criteria included males between the ages of 18 and 80 with a height of 165–186 cm, weight of 64–106 kg and a body mass index (BMI) of 18–35, with no positive serology for transmissible disease (HIV, and Hepatitis A, B and C). In addition, each specimen was also screened for bone mineral density using standard lumbar spine dual-energy x-ray absorptiometry (DEXA)

with an acceptance criterion of T-score within − 1 to 2.5 indicating a normal bone mineral density [9]. During preparation, the ribs, musculature, fat, and periosteum were carefully removed from the thoracolumbar spines to preserve the osteoligamentous structure, and the specimen was continuously hydrated through wrapping of saline-soaked gauze and direct application of physiological saline. This allowed for placement of acoustic sensors, accelerometer, and strain gauges as described in Ortiz-Paparoni et al. [14]. This preparation procedure has been shown to not damage or otherwise affect the mechanical properties of bones, ligaments, and the annulus fibrosus of the intervertebral discs (IVDs) [6, 20, 24]. The lumbar spines were fixed to aluminum cups using poly methyl methacrylate (PMMA) and a high-density urethane casting resin (Golden West Mfg., Inc., Grass Valley, CA 95945) at the superior (T12) and inferior ends (S1) to facilitate rigid attachment to a Materials Testing Machine (MTS®, Eden Prairie, MN, USA). Following the procedures outlined in Ortiz-Paparoni et al. [14], specimens were subjected to physiological preconditioning (300 cycles of 1% engineering strain at 1 Hz) and loaded twice under non-injurious compression profiles, allowing 10 minutes of viscoelastic recovery between loading profiles. The specimens were loaded from the inferior end (S1) via the servohydraulic ram in displacement control, while the superior end (T12) was fixed to the stationary end of the MTS crosshead. To appropriately integrate the data sets and expand the combined loading injury criterion, displacement targets for non-injurious and injurious loading were informed by Ortiz-Paparoni et al. [14]. Furthermore, the stiffness of the specimen, determined by the displacement at the inferior end and the force at the superior end, was used to assess behavior repeatability and mechanical integrity after testing. Once the non-injurious test battery was completed and the mechanical integrity of the specimens was confirmed, specimens were loaded to failure at an average velocity and time to peak displacement of 6.5 ± 2.5 m/s and 36.7 ± 5.6 ms, respectively.

The general test setup (Fig. 2) included a superior six-axis load cell (MC5-6-5000; AMTI, Watertown, MA) with a 22.2 KN max load to measure axial compression forces and bending moments during loading at the fixed crosshead of the MTS. Two strain gauges were used, (one of Model EA-06-062AQ-350/P, CEA-13-250UW-350 or C2A-06-062LW-350, VPG Micro Measurements, Wendell, NC) with one strain gauge glued to each of the L2 and L4 vertebral bodies. As with force and moment collection, strain gauges were sampled at 100 kHz and filtered with a 3000 Hz, phaseless 4th-pole low pass Butterworth filter to allow frequencies higher than those outlined in SAE J211 [19]. Twelve acoustic sensors (Mistras S9225, Physical Acoustic Corporation, 300–1800 KHz) were instrumented

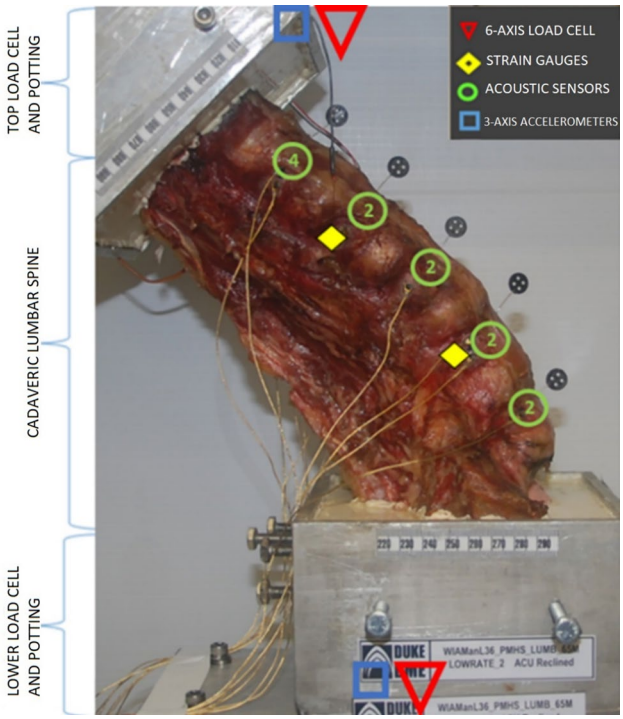

Fig. 2 Right side-view of test setup for LSPN36. The lumbar spine specimen is in the ACU reclined position and instrumentation has been identified

on the vertebral bodies of interest to assist with the assessment and timing of fracture. Four acoustic sensors were glued to the L1 vertebral body, and two were glued to each of the remaining vertebral bodies (L2–L5).

An internal linear variable differential transformer (LVDT; Serial Number 227, MTS, Eden Prairie, MN) measured displacements on the servohydraulic actuator applying the compression profile to the specimen. Displacement was collected at 100 kHz and filtered with a 3000 Hz, phaseless 4th-pole low pass Butterworth filter. Finally, necropsy and microCT imaging was performed after the failure test on the specimen to determine injury outcome. To provide interval-censored data for the injury analysis [8], the timing of injury during the loading phase of the failure test was assessed by means of strain gauges and acoustic emissions. It is important to note that only acoustic emissions of a certain frequency range [21] were recognized to be indicative of fracture, requiring a band pass filter comprising a phaseless Butterworth 4th order high pass at 100 KHz and a Butterworth 4th order low pass filter at 1 MHz. To further isolate acoustic signals, Morlet wavelet frequency identification was used to identify signals at 1.5× of the noise maximum. To further complement and confirm the initiation of fracture indicated by the acoustic data, sudden decreases in strain response of the strain gauges were also assessed.

Injury was defined as one or more vertebral body fractures. For injured specimens, the censoring interval was bounded between the metric value, at the onset of an acoustic emission and its peak value. Specimens that had injuries other than vertebral body fracture were right censored using the peak value of the metric during the injury test. Minitab 19 (Minitab Inc., State College, PA, USA) was used to assess the results of these tests and conduct the survival analysis for establishing the injury criterion. To maintain consistency across the experimental groups and allow a straightforward integration of the data sets, the expanded combined loading injury criterion was determined using the resultant force (F_r) of the sagittal plane (antero-posterior force, F_x, and superior-inferior force, F_z) at the T12/L1 joint. Similar to the combined loading injury metric (κ) proposed in the LIC study [14], the expanded combined loading injury metric (λ) was defined as:

$$\lambda = \frac{F_r}{F_{r,crit}} + \frac{M_y}{M_{y,crit}} \tag{1}$$

Further, the data set was also subjected to the moment decorrelation procedure used in Ortiz-Paparoni et al. [14]. Three parametric distributions were evaluated to determine the injury risk. The cumulative density functions that describe the three parametric distributions evaluated correspond to:

$$Lognormal: \frac{1}{2} + \frac{1}{2}\left(\operatorname{erf}\left(\frac{\ln(\lambda) - \mu}{\sigma\sqrt{2}}\right)\right) \tag{2}$$

$$Loglogistic: \frac{1}{\left(1 + exp\left[-\frac{\ln(\lambda)-\mu}{\sigma}\right]\right)} \tag{3}$$

$$Weibull: 1 - e^{-\left(\frac{\lambda}{\sigma}\right)^{\mu}} \tag{4}$$

With the location (μ) and scale (σ) parameters estimated through maximum likelihood. The distribution with the lowest Anderson-Darling (AD) coefficient (which assesses whether a given sample is drawn from a given distribution; a lower score is a better distribution fit) was selected as the best representation of the injury risk [1]. In contrast with the LIC, the Anderson-Darling coefficient fit was selected as the optimization target over the minimization of the normalized confidence interval size (NCIS) to ensure that the fit of the data was the primary feature of the injury risk model. Similar to the LIC, for a given test, a peak value of the combined loading metric (λ) exists and it is given by $F_{r,\text{crit}}$ and $M_{y,\text{crit}}$. The critical values are ideally identified through tests with pure axial loading and pure bending loading which are currently unknown for the proposed test conditions. However, the optimization of the AD coefficient allows the determination of the critical values by first starting with an initial approximation, followed by a calculation of λ for the failure tests. Then a λ metric is calculated for known non-failure points based on acoustic and strain gauge data and a risk function is derived from the parametric distribution based on interval censoring using the previously identified injury and non-injury points. The AD coefficient is evaluated for the resulting distribution and then $F_{r,\text{crit}}$ and $M_{y,\text{crit}}$ are optimized through a line search algorithm until the AD coefficient is minimized [28]. Finally, to evaluate the suitability of the 15 specimens in comparison to the 75-specimen data set, the results of the new dataset were weighted up to 5 times (5X) the value of the old tests. This adjustment was made to ensure the new tests were numerically equivalent to the old tests.

Results

A total of fifteen tests were performed in the expanded moment posture range, 4 in each of the ACU reclined, flexed reclined, and flexed nominal postures, and 3 in the intermediate posture. These tests resulted in 13 single or multi-level vertebral body fractures (1-2 fractures per specimen), with 2 specimens presenting an intervertebral disc injury, and a neural arch fracture. The fifteen specimens had a mean ± standard deviation (SD) age, weight, height, and BMI of 64 ± 9 years, 80 ± 17 kg, 175 ± 7 cm, and 26 ± 4 kg/m^2, respectively. Representative forces and moments (F_z, F_x, F_r, M_y) for the initiation of fracture and at maximum axial force were determined and are given in Table 1. Fracture initiation was determined by acoustic emissions and strain gauge data where available. However, fracture initiation was not clearly identified in two scenarios. In these cases, the non-injury tests values were used to define the lower bound of the censoring interval.

Compared to the nominal range of posture previously evaluated [14], the data set presented lower correlation values between the axial force and bending moment (Fig. 3). Decorrelation of M_y by translating the center of rotation in the antero-posterior direction towards the effective center of motion allowed the evaluation of independent effects on stress from M_y and F_z. Displacements for the moment decorrelation are shown in Fig. 4.

The optimized AD fit coefficients for the parametric distributions evaluated were 0.918, 0.422, and 0.517 for the Weibull, Loglogistic, and Lognormal distributions, respectively. With the lowest AD coefficient, the loglogistic distribution was selected as the best representation of injury risk, resulting in optimized critical values of $F_{r,\text{crit}} = 6011$

Table 1 Summary of F_z-based peak values at the center of the T12/L1 IVD for the expanded test series

Test ID	Fracture initiation Acoustic + strain gauge onset				Value at peak axial force				VB fx
	F_z (N)	M_y (Nm)	F_x (N)	F_r (N)	F_z (N)	M_y (Nm)	F_x (N)	F_r (N)	
LSPN33	–	–	–	–	4477	103	3508	5688	0
LSPN34	2803	41	2393	3686	3211	54	1886	3724	1
LSPN35	3873	33	4048	5603	4850	23	3450	5952	1
LSPN36	2796	22	2389	3678	3490	18	2068	4057	1
LSPN37	NI	NI	NI	NI	3694	2	1774	4098	1
LSPN38	5199	138	1572	5432	6626	5	2583	7112	1
LSPN39	6933	114	2009	7219	7006	138	1882	7255	1
LSPN40	4513	111	1267	4688	5866	134	1339	6016	1
LSPN41	NI	NI	NI	NI	4473	76	4126	6085	1
LSPN42	5581	92	1348	5742	5967	66	2708	6553	1
LSPN43	6205	29	2014	6524	7395	28	2045	7673	1
LSPN44	4663	61	1498	4898	4732	69	1462	4952	1
LSPN45	–	–	–	–	7958	206	3609	8738	0
LSPN46	6673	121	4018	7790	7030	17	3012	7648	1
LSPN47	6475	84	3537	7378	6794	11	3096	7466	1

NI denotes that non-injury test values were used as the lower bound of the censoring interval, 1 denotes the presence of single or multiple vertebral body fractures (VB fx), 0 denotes the absence of VB fx, and "–" denotes the absence of VB fx metrics. Note that the upper and lower bounds of the interval censored data are defined by the value at peak axial force and the value at the fracture initiation, respectively. Specimens that did not present vertebral body fractures were designated as right censored

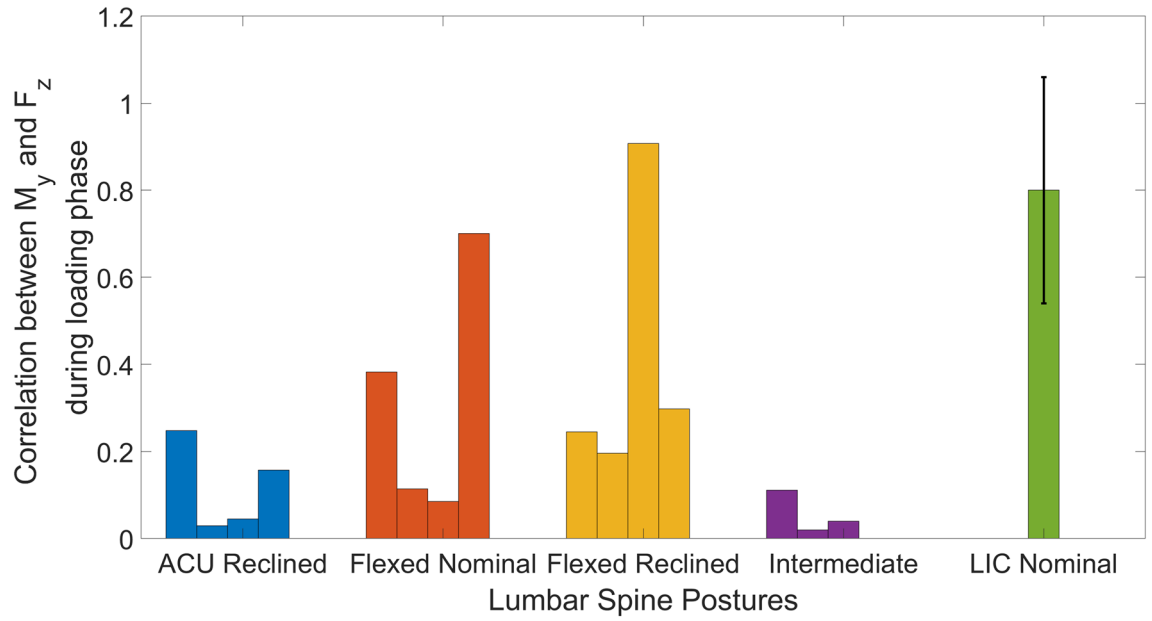

Fig. 3 Correlation of F_z and M_y for 15 expanded range lumbar tests. Correlations between axial force and moment are generally smaller for the more off-axial tests (ACU Reclined and Intermediate). Correlations are generally lower than those in the previous 75 nominal posture range (LIC mean correlation = 0.8 ± 0.26; ECLIC mean correlation = 0.24 ± 0.26)

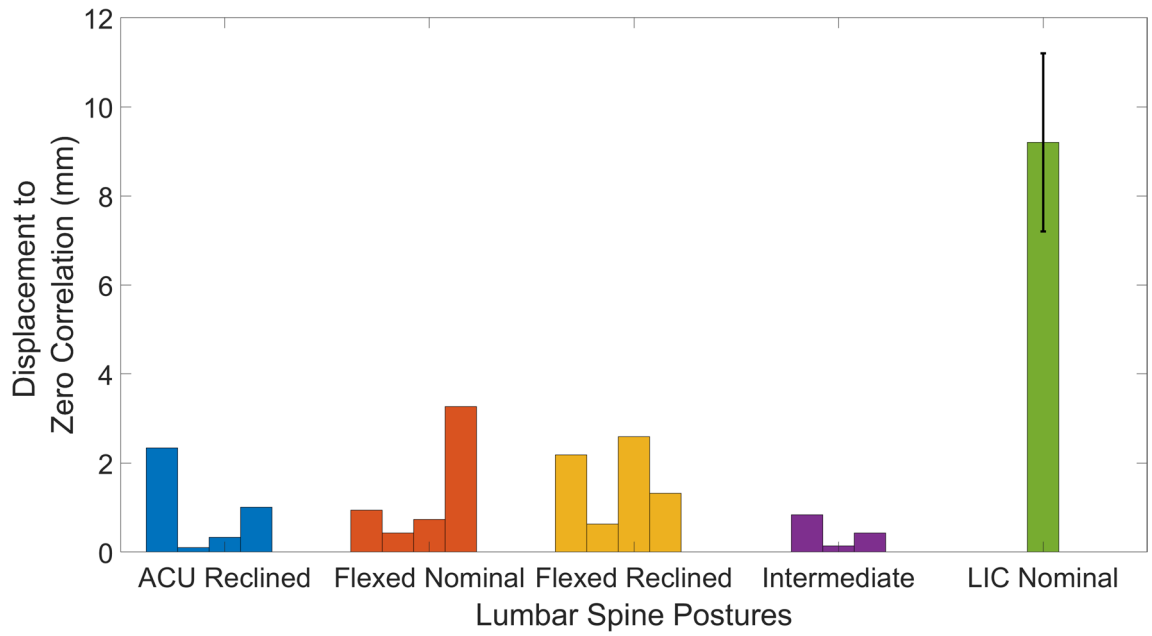

Fig. 4 Posterior translations to the effective center of rotation that minimize correlation between F_z and M_y for the expanded data set. Compared to previous data set (LIC median and standard error displacement of 9.2 ± 2 mm, respectively), the extended postures required a smaller translation to achieve F_z and M_y decorrelation (ECLIC median and standard error displacement of 0.84 ± 0.25 mm, respectively).

N, and $M_{y,crit} = 904$ Nm, with location (μ) and scale (σ) parameters equal to 0 and 0.1797, respectively. The Loglogistic injury risk (Fig. 5) is given by Eq. 5 and selected values of the injury risk are given in Table 2.

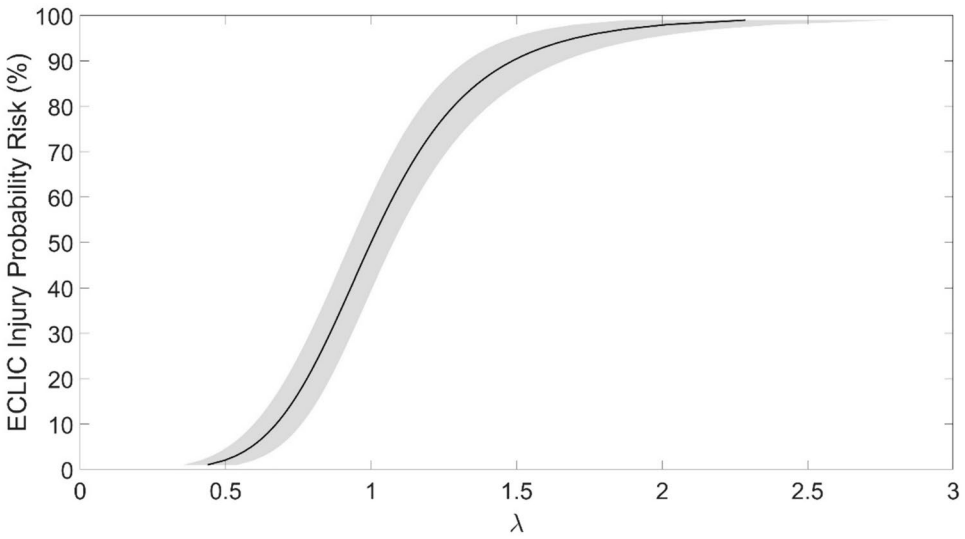

Fig. 5 Lumbar spine vertebral body fracture injury risk for the expanded combined loading injury criterion (ECLIC). The combined metric λ consists of a combination of the T12/L1 resultant force and moment fitted to a Loglogistic distribution (center black line) with 95% confidence intervals (shaded area). The proposed injury criterion (ECLIC) includes 15 new specimens with augmented eccentric loading to the previously established combined loading injury criterion (LIC), totaling 90 specimens evaluated in the development of ECLIC

Table 2 Selected injury risk values for the T12/L1 resultant force and moment combined loading metric (λ)

Risk Level	λ	Lower 95% CI	Upper 95% CI	NCIS
0.05	0.59	0.51	0.68	0.30
0.1	0.67	0.60	0.76	0.24
0.2	0.78	0.71	0.86	0.19
0.3	0.86	0.79	0.93	0.17
0.4	0.93	0.86	1.00	0.15
0.5	1.00	0.93	1.08	0.15
0.6	1.08	1.00	1.16	0.15
0.7	1.16	1.08	1.26	0.16
0.8	1.28	1.17	1.40	0.18
0.9	1.48	1.33	1.66	0.22
0.95	1.70	1.48	1.95	0.27

$$ECLIC = \frac{1}{\left(1 + exp\left[-\frac{\ln(\lambda)-0}{0.1797}\right]\right)} \tag{5}$$

$$\lambda = \frac{F_r}{6011} + \frac{M_y}{904} \tag{6}$$

Since the new expanded posture tests ($n = 15$) comprise a fraction of the total number of tests ($n = 90$), weightings were explored to determine if the effect of the new tests was qualitatively different than the existing tests. Anderson-Darling coefficients for 5× augmented data set fit indicate that the statistical fit tests improve with the new weightings for all the distributions evaluated. The NCIS also qualitatively improves with the 5× weighting (Fig. 7B). In contrast, the effect of the 5× analysis on the mean risk is minimal (Fig. 7A).

Discussion

The objective of this study was to expand the applicability of the previously established lumbar spine injury criterion (LIC) [14] to a larger range of postures and generate a model of injury risk for a combined loading scenario based on cadaveric data. The analysis methods followed best practices in the injury biomechanics community and maintained continuity with the previously developed criterion. A new range of postures with increased flexion/extension of the lumbar spine (Fig. 1) was included to the expanded criterion (ECLIC) and augmented its applicability within the seated Soldier environment. The combined metric using the sagittal T12/L1 resultant force and moment was the recommended metric to evaluate vertebral body fracture risk and is extended to and beyond one standard deviation of the seated Soldier study nominal posture [17].

In contrast with the previous axial-compression dominated data, the current dataset correlations between F_z and M_y are often small (Fig. 3), reflecting relatively independent contributions to the stress state in the spine (ECLIC mean correlation $= 0.24 \pm 0.26$ vs LIC mean correlation $= 0.8 \pm 0.26$). In the previous study, the majority of the nominal posture range tests show highly correlated data owing to differences between the effective center of rotation and the assumed center in the middle of the T12/L1 intervertebral disc [14]. The lower distance to the effective center of rotation for the expanded data set (Fig. 4), when compared to the nominal posture range, agrees with the smaller correlation observed between F_z and M_y for the expanded postures (LIC median and $SE = 9.2 \pm 2$ mm vs. ECLIC median and $SE = 0.84 \pm 0.25$ mm). Even though $F_z - M_y$ correlations and displacements to achieve de-correlation were smaller in the current dataset, the practice of moment decorrelation remains relevant. This is essential for integrating with the

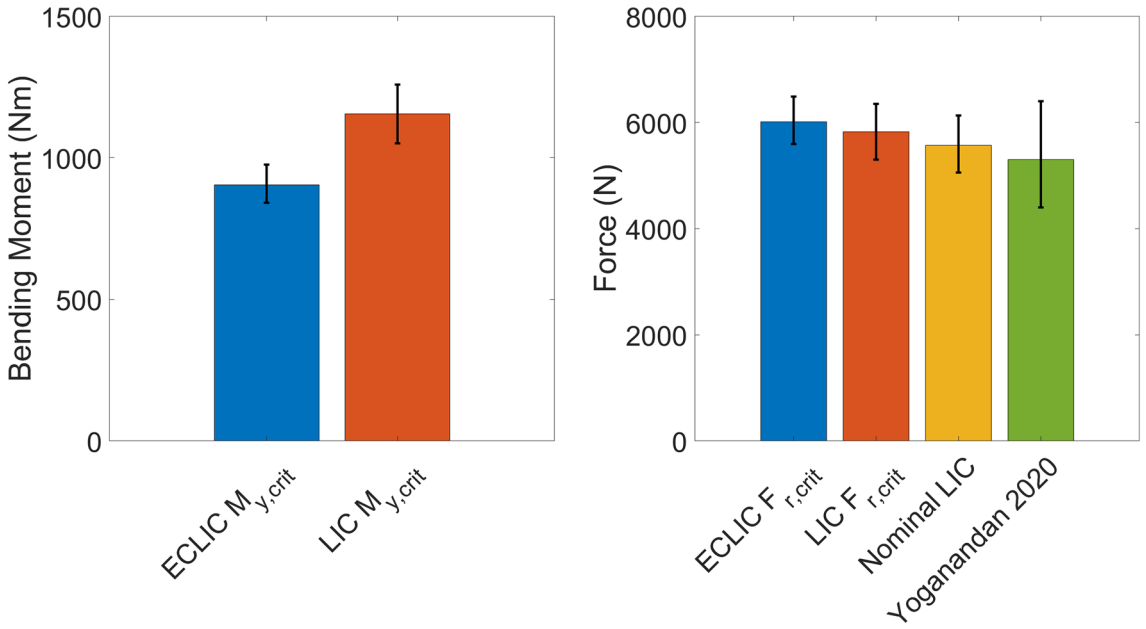

Fig 6. Critical values for the combined loading metric. (Left) The increased contribution of the bending moment to the expanded injury criterion is observed through the reduced bending moment critical value (ECLIC $M_{y,\text{crit}} = 904$ Nm) compared to that reported by Ortiz-Paparoni et al. [14] (LIC $M_{y,\text{crit}} = 1155$ Nm). (Right) The expanded injury criterion presents the smaller resultant force contribution among other lumbar spine injury criteria for dynamic compression

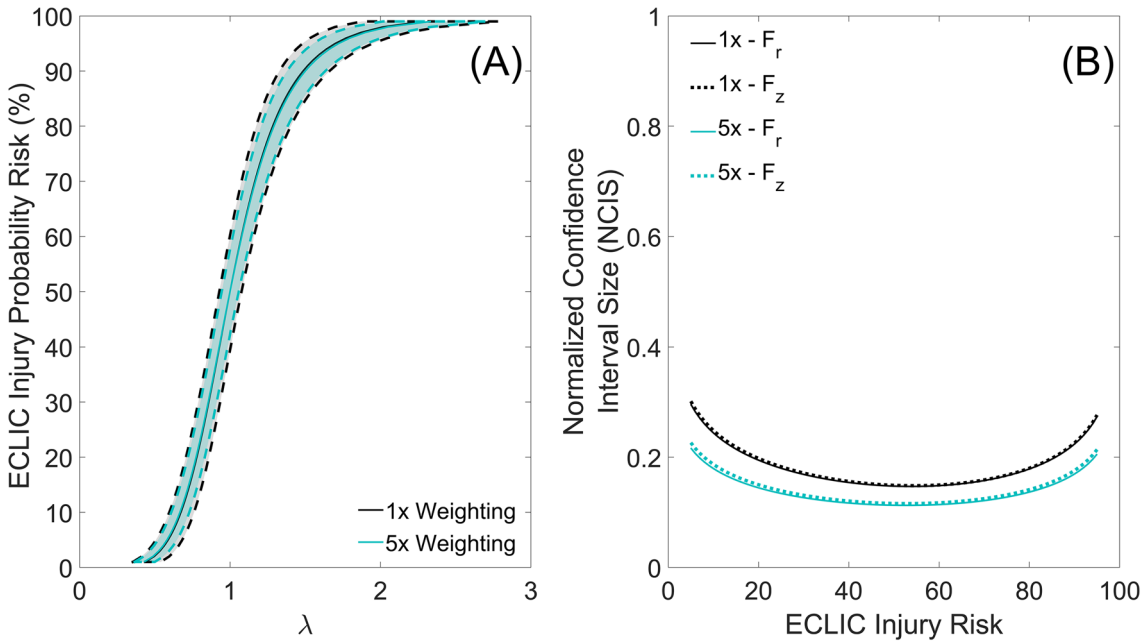

Fig. 7 **A** Loglogistic injury risk for 1× and 5× weighting. The mean curves for F_r − 5× and F_r − 1× weighted are indistinguishable at this scale though the 5× confidence intervals are improved in the 5× analysis due to the artificial increase of the number of specimens. **B** NCIS values for Loglogistic distribution for F_z and F_r-based injury risk models. The 5× analysis is generally better than the 1× analysis

existing injury criterion and for accounting for the independent effects of axial force and bending moment on the stress state of the specimens.

The bending moment in the additional 15 specimens presents a higher contribution than that previously evaluated in the nominal posture range (Eq. 6). When combining

the extended range of evaluated postures with the original dataset [14], the optimization of the Anderson-Darling coefficient for the ECLIC development resulted in a smaller critical M_y value (ELIC $M_{y,\text{crit}} = 904 \pm 70$ Nm vs. LIC $M_{y,\text{crit}} = 1155 \pm 100$ Nm). Dividing by a lower critical value in the injury metric calculations results in a larger contribution of moment to the injury risk. This reduction highlights the expanded contribution of the bending moment to the one captured by the previously developed injury criterion (Fig. 6, left), which is also observed with the decreased contribution of the resulting compressive force (LIC $F_{r,\text{crit}} = 5.8 \pm 0.5$ kN vs. ECLIC $F_{r,\text{crit}} = 6 \pm 0.5$ kN). Though no significant differences were observed, $F_{r,\text{crit}}$ for the expanded dataset is higher compared to other 50% injury risk resultant force metrics at the superior end of the lumbar spine (T12/L1) in similar studies (ECLIC $F_{r,\text{crit}} = 6 \pm 0.5$ kN, Nominal $LIC = 5.6 \pm 0.5$ kN [14], Yoganandan 2020 $F_r = 5.4 \pm 1$ kN [31]) (Fig. 6, right). This further reinforces the expansion of the moment contribution to the proposed injury criterion (ECLIC). While the combined metric was developed for UBB compressive profiles, it could be applied to scenarios with loading vectors that emphasize underbody forces, which can be found both in the civilian population in complex motor vehicle accidents, as well as in military scenarios such as pilot ejections, or rotary wing accidents. By accounting for contributions of bending moment and resultant forces to the injury risk, the combined metric can represent a framework that may become the generic metric for injury predictions in general dynamic loading. The associated distribution function which best represented the data, with an optimized Anderson-Darling coefficient, was a Loglogistic distribution. While the expansion of the injury criterion provides valuable insights into lumbar spine injury risk, it is important to note that the developed criterion specifically assesses the risk of a single or multi-level vertebral body fracture occurring during a dynamic compressive event. Therefore, additional studies are needed to develop an injury probability risk for different injury types across multiple vertebral bodies, injuries to intervertebral disc, or injuries to the spinous processes.

Due to the discrepancy in the number of specimens available between the nominal and expanded posture ranges ($n = 75$ vs. $n = 15$), alternative weighting for the expanded posture data set was explored. Overall, though there is an improvement in NCIS in the 5× analysis (Fig. 7B), the lack of qualitative effect on the mean curve suggests that the 1× analysis is an adequate representation of the range of postures included in this study and should be the analysis on which the injury criterion is based (Fig. 7A). The expanded combined metric (λ) of 1.0 represents a 50% chance of a single or multi-level vertebral body fracture (Fig. 5). Approximately 1.7 and 0.59 represent a 95 and a 5% chance of the same injury, respectively.

While this work presents the first broadly applicable combined loading injury criterion for lumbar vertebral body fracture in a spine positioned in a range of seated postures subjected to UBB loading conditions, it is not without its limitations, and other recent studies address similar fundamental questions on spine combined loading through a different perspective. Tushak et al. examined a different method of modeling lumbar spine behavior under bending-dominated combined loading, simulating the lumbar spine as a beam [25]. While a significantly smaller force was required to reach 50% injury risk in the beam model relative to Ortiz-Paparoni et al, Tushak et al. included both male and female functional spinal units in the study, whereas both Ortiz-Paparoni et al. and this study tested thoraco-lumbar male cadaver spines (T12-S1) [14, 25]. Discrepancies in failure tolerance between the studies could be attributed to differences in behavior between FSUs and whole lumbar spines [15], the loading regime prescribed in each test series (moment-dominated for Tushak vs. axial-dominated for Ortiz-Paparoni), and sex of the sampled population. Men and women present different material characteristics including bone mineral density, particularly as age increases, as women were found to have decreased cortical bone area and a substantially faster decline of cortical bone density (3×) per year compared to men, despite an overall increase in total bone area [18]. Further, bone mineral density in the lumbar spine has been examined in osteoporosis studies [27, 29] and similarly greater declines were seen in older women relative to men. These differences may affect the predictive risk of injury for the models used in Tushak et al. and Ortiz-Paparoni et al., and further studies are needed to examine the effect of age and sex on the injury criterion.

This study also possesses physical limitations: the maximum moment in the dataset was 487 Nm after minimizing the $F_z - M_y$ correlation and the maximum M_y (Nm)/F_z (kN) ratio in the current dataset was extended from the nominal posture 0.06 to 0.1. Therefore, the strict applicability of this injury criterion is for scenarios with less than 487 Nm of M_y and can be expanded beyond a 0.06 M_y/F_z ratio but kept in scenarios where the ratio is less than 0.1. The recommended applicability of this HIPC is to scenarios where the $|F_x|/F_r$ ratio is less than 50%. Shear force contributions are also increased with this expanded dataset. This model also assumes that pure flexion and pure extension moments to failure are the same or of similar magnitude, but these factors are observed to not be the same. Tension contributions are also not examined under this injury criterion being that testing examined only the flexion/compression quadrant. Additionally, this study does not examine lateral or torsional bending or moments (e.g., M_x and M_z, respectively) or transverse forces (e.g., F_y) despite the likelihood of these factors being present in a military vehicle scenario. These factors

are thus likely important in considering vehicular loading contexts and should be considered for future work.

The expanded criterion (ECLIC) enhances its relevance by increasing the range of applicability across lumbar spine flexion/extension postures. Key findings emphasize the significant contribution of the bending moment that resulted from the incorporation of the expanded dataset, as evidenced by a lower critical M_y value and a higher critical F_r. These results underscore the expanded scope of ECLIC in assessing vertebral body fracture risk in the lumbar spine during dynamic compression events.

Acknowledgements This work was sponsored by the United States Army Research Lab and The U.S. Army Combat Capabilities Development Command (DEVCOM) Analysis Center in support of the Warrior Injury Assessment Manikin (WIAMan) Program. The authors gratefully acknowledge the contributions of the WIAMan Engineering Office. The views expressed are those of the authors and do not necessarily represent the official position or policy of the U. S. Government, the Department of Defense (or its branches), or the Department of the Army.

Funding This work was sponsored by the United States Army Research Lab and The U.S. Army Combat Capabilities Development Command (DEVCOM) Analysis Center in support of the Warrior Injury Assessment Manikin (WIAMan) Program. The authors gratefully acknowledge the contributions of the WIAMan Engineering Office. The views expressed are those of the authors and do not necessarily represent the official position or policy of the U. S. Government, the Department of Defense (or its branches), or the Department of the Army.

Declarations

Competing Interests The authors have no conflicting interest to report.

References

1. Anderson, T. W., and D. A. Darling. A test of goodness of fit. *J Am Stat Assoc.* 1954. https://doi.org/10.2307/2281537.
2. Blair, J. A., J. C. Patzkowski, A. J. Schoenfeld, J. D. Cross Rivera, E. S. Grenier, R. A. Lehman Jr., and J. R. Hsu. The skeletal trauma research consortium (STReC). Spinal column injuries among Americans in the global war on terrorism. *J Bone Joint Surg Am.* 2012. https://doi.org/10.2106/JBJS.K.00502.
3. Danelson, K., L. Watkins, J. Hendricks, P. Frounfelker, K. Pizzolato-Heine, R. Valentine, K. Loftis, WIAMan Case Review Team. Analysis of the frequency and mechanism of injury to warfighters in the under-body blast environment. *Stapp Car Crash J.* 2018. https://doi.org/10.4271/2018-22-0014.
4. den Ouden, L. P., A. J. Smits, A. Stadhouder, R. Feller, J. Deunk, and F. W. Bloemers. Epidemiology of spinal fractures in a level one trauma center in the Netherlands: a 10 years review. *Spine.* 2019. https://doi.org/10.1097/BRS.0000000000002923.
5. Duma, S. M., A. R. Kemper, D. M. McNeely, P. G. Brolinson, and F. Matsuoka. Biomechanical response of the lumbar spine in dynamic compression. *Biomed Sci Instrum.* 42:476–481, 2006.
6. Galante, J. O. Tensile properties of the human lumbar annulus fibrosus. *Acta Orthop Scand.* 1967. https://doi.org/10.3109/ort.1967.38.suppl-100.01.
7. Kang, D. G., R. A. Lehman Jr., and E. J. Carragee. Wartime spine injuries: understanding the improvised explosive device and biophysics of blast trauma. *Spine J.* 2012. https://doi.org/10.1016/j.spinee.2011.11.014.
8. Klein, J. P., and M. L. Moeschberger. Survival analysis: techniques for censored and truncated data, 2nd ed. New York: Springer, 2003.
9. Krugh M, Langaker MD. Dual Energy Xray Absorptiometry. In: StatPearls. National Library of Medicine. 2023. https://www.ncbi.nlm.nih.gov/books/NBK519042/. Accessed 7 Feb 2023.
10. Leucht, P., K. Fischer, G. Muhr, and E. J. Mueller. Epidemiology of traumatic spine fractures. *Injury.* 2009. https://doi.org/10.1016/j.injury.2008.06.040.
11. Loftis, K., K. Sandora, and D. Drewry III. Introduction to the WIAMan biomechanics program. *Ann Biomed Eng.* 49:2973–2974, 2021.
12. Loftis, K. L., E. L. Mazuchowski, M. C. Clouser, and P. J. Gillich. Prominent injury types in vehicle underbody blast. *Mil Med.* 2019. https://doi.org/10.1093/milmed/usy322.
13. Niemi-Nikkola, V., N. Saijets, H. Ylipoussu, P. Kinnunen, J. Pesälä, P. Mäkelä, M. Alen, and V. A. Kallinen. Traumatic spinal injuries in Northern Finland. *Spine*. 2018. https://doi.org/10.1097/BRS.0000000000002214.
14. Ortiz-Paparoni, M., J. Op 't Eynde, J. Kait, B. Bigler, J. Shridharani, A. Schmidt, C. Cox, C. Morino, F. Pintar, N. Yoganandan, J. Moore, J. Y. Zhang, and C. R. Bass. The human lumbar spine during high-rate under seat loading: a combined metric injury criteria. *Ann Biomed Eng*. 49:3018–3030, 2021.
15. Ortiz-Paparoni MA, Pigue M, Bass CR. Building a Whole Spine from Segments: Lumbar Spine Response during Dynamic Compression. In: IRCOBI Proceedings. International Research Council on Biomechanics of Injury. 2020. http://www.ircobi.org/wordpress/downloads/irc20/pdf-files/86.pdf. Accessed 13 Dec 2022.
16. Ramasamy, A., S. D. Masouros, N. Newell, A. M. Hill, W. G. Proud, K. A. Brown, A. M. Bull, and J. C. Clasper. In-vehicle extremity injuries from improvised explosive devices: current and future foci. *Philos Trans R Soc B: Biol Sci*. 2011. https://doi.org/10.1098/rstb.2010.0219.
17. Reed MP, Ebert SM. The seated soldier study: posture and body shape in vehicle seats. In: Transportation Research Institute (UMTRI). University of Michigan Library. 2013. https://deepblue.lib.umich.edu/handle/2027.42/109725. Accessed 7 Oct 2022.
18. Russo, C. R., F. Lauretani, S. Bandinelli, B. Bartali, A. Di Iorio, S. Volpato, J. M. Guralnik, T. Harris, and L. Ferrucci. Aging bone in men and women: beyond changes in bone mineral density. *Osteop Int*. 2003. https://doi.org/10.1007/s00198-002-1322-y.
19. SAE S. J211-1 instrumentation for impact test—Part 1—Electronic instrumentation. SAE International 2007.
20. Sedlin, E. D., and C. Hirsch. Factors affecting the determination of the physical properties of femoral cortical bone. *Acta Orthop Scand*. 1966. https://doi.org/10.3109/17453676608989401.
21. Shridharani, J. K., M. A. Ortiz-Paparoni, J. Op 't Eynde, and C. R. Bass. Acoustic emissions in vertebral cortical shell failure. *J Biomech*. 2021. https://doi.org/10.1016/j.jbiomech.2021.110227.
22. Spurrier, E., I. Gibb, S. Masouros, and J. Clasper. Identifying spinal injury patterns in underbody blast to develop mechanistic hypotheses. *Spine.* 2016. https://doi.org/10.1097/BRS.0000000000001213.
23. Stemper, B. D., S. Chirvi, N. Doan, J. L. Baisden, D. J. Maiman, W. H. Curry, N. Yoganandan, F. A. Pintar, G. Paskoff, and B. S. Shender. Biomechanical tolerance of whole lumbar spines in straightened posture subjected to axial acceleration. *J Orthop Res*. 2018. https://doi.org/10.1002/jor.23826.
24. Tkaczuk, H. Tensile properties of human lumbar longitudinal ligaments. *Acta Orthop Scand*. 1968. https://doi.org/10.3109/ort.1968.39.suppl-115.01.

25. Tushak, S. K., B. D. Gepner, J. L. Forman, J. J. Hallman, B. Pipkorn, and J. R. Kerrigan. Human lumbar spine injury risk in dynamic combined compression and flexion loading. *Ann Biomed Eng*. 51:1216–1225, 2023.
26. Wang, H., Y. Zhang, Q. Xiang, X. Wang, C. Li, H. Xiong, and Y. Zhou. Epidemiology of traumatic spinal fractures: experience from medical university–affiliated hospitals in Chongqing, China, 2001–2010. *J Neurosurg: Spine.* 2012. https://doi.org/10.3171/2012.8.SPINE111003.
27. Warming, L., C. Hassager, and C. Christiansen. Changes in bone mineral density with age in men and women: a longitudinal study. *Osteop Int.* 13:105–112, 2002.
28. Wolfe, P. Convergence conditions for ascent methods. *SIAM Rev.* 11:226–235, 1969.
29. Wright, N. C., A. C. Looker, K. G. Saag, J. R. Curtis, E. S. Delzell, S. Randall, and B. Dawson-Hughes. The recent prevalence of osteoporosis and low bone mass in the United States based on bone mineral density at the femoral neck or lumbar spine. *J Bone Mineral Res*. 2014. https://doi.org/10.1002/jbmr.2269.
30. Yoganandan, N., N. DeVogel, J. Moore, F. Pintar, A. Banerjee, and J. Zhang. Human lumbar spine responses from vertical loading: ranking of forces via Brier score metrics and injury risk curves. *Ann Biomed Eng*. 48:79–91, 2020.
31. Yoganandan, N., J. Moore, N. DeVogel, F. Pintar, A. Banerjee, J. Baisden, J. Y. Zhang, K. Loftis, and D. Barnes. Human lumbar spinal column injury criteria from vertical loading at the base: applications to military environments. *J Mech Behav Biomed Mater*. 2020. https://doi.org/10.1016/j.jmbbm.2020.103690.
32. Yoganandan, N., J. Moore, J. Humm, M. Philippens, and T. Westerhof. Hybrid III dummy lumbar spine responses under vertical impact loading. *Traffic Injury Prev.* 2022. https://doi.org/10.1080/15389588.2022.2124812.
33. Yoganandan, N., B. D. Stemper, J. L. Baisden, F. A. Pintar, G. R. Paskoff, and B. S. Shender. Effects of acceleration level on lumbar spine injuries in military populations. *Spine J*. 2015. https://doi.org/10.1016/j.spinee.2013.07.486.

Authors and Affiliations

Maria Ortiz-Paparoni[1] · Joost Op 't Eynde[1] · Christopher Eckersley[1] · Concetta Morino[2] · Mitchell Abrams[1] · Derek Pang[1] · Jason Kait[1] · Frank Pintar[3] · Narayan Yoganandan[4] · Jason Moore[4] · David Barnes[5] · Kathryn Loftis[6] · Cameron R. Bass[1]

✉ Maria Ortiz-Paparoni
maortizpaparoni@gmail.com

Joost Op 't Eynde
joost.opteynde@duke.edu

Christopher Eckersley
christopher.eckersley@duke.edu

Concetta Morino
concetta.morino@duke.edu

Mitchell Abrams
mitchell.abrams@duke.edu

Derek Pang
derek.pang@duke.edu

Jason Kait
jkait@duke.edu

Frank Pintar
fpintar@mcw.edu

Narayan Yoganandan
yoga@mcw.edu

Jason Moore
jmoore@mcw.edu

David Barnes
david.r.barnes63.ctr@army.mil

Kathryn Loftis
kathryn.l.loftis2.civ@army.mil

Cameron R. Bass
dale.bass@duke.edu

[1] Department of Biomedical Engineering, Duke University, Durham, NC 27708, USA

[2] Department of Mechanical Engineering and Material Science, Duke University, Durham, NC 27708, USA

[3] Joint Department of Biomedical Engineering, Marquette University and the Medical College of Wisconsin, Milwaukee, WI 53226, USA

[4] Department of Neurosurgery, Medical College of Wisconsin, Milwaukee, WI 53226, USA

[5] Survice Engineering Co., Belcamp, MD 21017, USA

[6] AFC DEVCOM Analysis Center, Aberdeen Proving Ground, MD 21005, USA